UFSM

CIÊNCIA e NATURA

ISSN 2179-460X
Acesso aberto

Ci. e Nat., Santa Maria, v. 43, e37, 2021 • https://doi.org/10.5902/2179460X39775
Submissão: 02/12/2020 • Aprovação: 15/04/2021 • Publicação: 19/05/2021

Meteorology

Daily Global and diffuse radiation in the Brazilian Cerrado-Amazon transition region

Radiação global e difusa diária na região de transição Cerrado-Amazônia brasileira

Tamara Zamadei[I], Adilson Pacheco de Souza[II], Frederico Terra de Almeida[II], João Franscisco Escobedo[III]

[I]Programa de Pós-Graduação em Física Ambiental, Universidade Federal de Mato Grosso, Cuiabá, MT, Brazil
[II]Instituto de Ciências Agrárias e Ambientais, Universidade Federal de Mato Grosso, Sinop, MT, Brazil
[III]Facudade de Ciências Agronômicas, Universidade Estadual Paulista, Botucatu, SP, Brazil

ABSTRACT

This study aimed to analyze the seasonal variations in atmospheric transmissivity and solar radiation (global and diffuse) on the horizontal surface in Sinop, Mato Grosso (MT) (11.865°S, 55.485°W, and altitude of 371 m) from 06/02/2011 to 12/31/2014. The values of diffuse radiation were measured using the Melo-Escobedo-Oliveira (MEO) shadow ring, with application of astronomical, geometric, and anisotropic correction factors. The analysis of atmospheric transmissivity was based on the classification of sky cover as cloudy, partly cloudy, partially clear, or clear. The diffuse radiation showed similar behavior to the radiation at the top of the atmosphere, reaching a maximum between October and April (rainy season), while the global radiation displayed higher levels during the dry season (May to September). The average daily global radiation ranged from 22.75±0.61 MJ m^{-2} d^{-1} in August to 16.44±1.45 MJ m^{-2} d^{-1} in January. In Sinop, cloudy and partly cloudy skies occurred on 45.6% of days and atmospheric transmissivity of global radiation was greater than 55% on 54.6% of days. The variations in diffuse radiation in the region were influenced by cloudiness and the concentration of biomass burning aerosol particles. The diffuse radiation can represent 8.02%–99.12% of the global radiation and 5.33%–29.01% of solar energy incident at the top of the atmosphere.
Keywords: Solar radiation; Clearness index; Shadow ring; Atmospheric attenuation

RESUMO

Este estudo objetivou analisar a variação sazonal da transmissividade atmosférica e radiação solar (global e difusa) incidente na superfície horizontal no município de Sinop, Mato Grosso (MT), (11,865°S; 55,485°W, e altitude de 371 m) de 02/06/2011 a 31/12/2014. Os valores de radiação difusa foram obtidos na utilização do anel de sombreamento Melo-Escobedo-Oliveira (MEO), com aplicação de fatores de correção astronômicos, geométricos e anisotrópicos. Para análise da variação da transmissividade atmosférica ao longo do ano estabeleceu-se a classificação da cobertura de céu como nublado,

parcialmente nublado, parcialmente aberto e aberto. A radiação difusa apresentou comportamento semelhante ao verificado no topo da atmosfera, com valores máximos durante o período de outubro a abril (estação chuvosa), já a radiação global apresentou maiores valores durante o período seco (Maio a Setembro). A média diária da radiação global atingiu valores de 22,75±0,61 MJ m^{-2} d^{-1} em Agosto a 16,44±1,45 MJ m^{-2} d^{-1} em Janeiro. Em Sinop, as coberturas de céu nublado e parcialmente nublado ocorreram em 45,6% dos dias e a transmissividade atmosférica da radiação global foi maior que 55% em 54,6% dos dias. As variações na radiação difusa na região foram influenciadas pela nebulosidade e concentração de aerossóis provenientes de queima de biomassa. A radiação difusa pode representar de 8,02%–99,12% da radiação global, e 5,33%–29,01% da radiação solar incidente no topo da atmosfera.
Palavras-chave: Radiação solar; Índice de claridade; Anel de sombreamento; Atenuação atmosférica

1 INTRODUCTION

Knowledge of solar radiation levels at the terrestrial surface is essential for energy use projects and research in a wide variety of fields, including agriculture (e.g., water use by plants and models of development or crop production); various aspects of atmospheric chemistry (e.g., the ozone layer and air quality), meteorology and climatology (e.g., hydric and energetic balance and climate-ocean interactions); energy efficiency and thermal comfort practices in architecture and construction (e.g., use of solar thermal energy as a potential alternative for water heating); and even solutions for water desalination (PEREIRA et al., 2006; SOUZA et al., 2012; CRUZ et al., 2020; SILVA; SHARQAWY, 2020).

The solar radiation that reaches the Earth's surface on the horizontal plane is called global radiation and can be divided into direct and diffuse components. Solar radiation is subject to atmospheric attenuation by reflection, absorption, and diffusion due to the interaction of electromagnetic waves with the constituent gases of the atmosphere, clouds and aerosols, which makes it difficult to predict (SOUZA; ESCOBEDO, 2013; RELVA et al., 2019).

Brazil has recently expanded its network of automatic weather stations, leading to a significant expansion in the number of routine measurements of solar radiation fluxes, because of financial conditions, a monitoring weather station typically measures global (with a pyranometer) mainly made in the horizontal plane, at several different time intervals (e.g., continuously, hourly, daily, monthly, or annually). Routine monitoring of the atmospheric attenuation components of solar radiation is conducted by universities and research institutes due to the costs involved in the acquisition and maintenance of the

instruments required (CODATO et al., 2008; MARTINS et al., 2008; ESCOBEDO et al., 2009; BORGES et al., 2010; PIACENTINI et al., 2011; VIANA et al., 2011; FURLAN et al., 2012; SALAZAR et al., 2020).

For diffuse measurements, the shadow ring method is the most used due to low costs, easy maintenance and optimal operation. The Melo-Escobedo-Oliveira (MEO) shadow ring method is low-cost and easy to operate and maintain (MELO, 1994). In the horizontal-plane measurements, the ring is held fixed and inclined on an angle equal to the site latitude. To compensate for the variation in solar declination and remain below the shadow produced by the ring, the pyranometer moves parallel to the plane of the local horizon on a movable base (OLIVEIRA et al., 2002; DAL PAI et al., 2016). However, its accuracy is affected by the portion of the sky blocked by the shadow ring, requiring geometric and atmospheric corrections (DAL PAI et al., 2014). This case, geometric correction is based on latitude, solar declination, ring's length and ring's width and doesn't take into account the circumsolar radiation.

According Dal Pai et al. (2016) this radiation is due to the scattering of direct radiation through small angles by the atmospheric particles (aerosols, water vapor, sky coverage) and is a result of the anisotropy of the radiation. These additional corrections may present temporal and spatial dependence due to the different sizes and concentrations of particulate matter in the atmosphere. The best representative parameter of anisotropic sky conditions is the atmospheric transmissivity (clearness index) "K_T" (ratio of global to extraterrestrial radiation).

A region in the northern part of Mato Grosso State presents an important type of vegetation cover: the transition forest between the Cerrado and the Amazon. Its climate is characterized by a well-defined seasonality with two seasons (a wet season and a dry season), which influence the levels of solar radiation at the surface. The sky cover is dependent on changes in atmospheric composition, which in turn depends on rainfall characteristics and the influence of biomass burning aerosols (ANDRADE et al., 2009; SOUZA et al., 2016; ROSSI; SANTOS, 2020).

Given the importance of understanding solar radiation and the lack of information on solar radiation in the Brazilian Midwest, this study aimed to evaluate the seasonality of monthly averages of global and diffuse radiation together with the global and diffuse atmospheric transmissivity coefficients in the municipality of Sinop, Mato Grosso (MT), in the Cerrado-Amazon transition region.

2 MATERIAL AND METHODS

2.1 Location and climate

The values of global and diffuse radiation on the horizontal surface were obtained from the Automatic Weather Station database of the Federal University of Mato Grosso, Campus of Sinop, located at 11.865°S, 55.485°W, and 371 m of altitude, from 06/02/2011 to 12/31/2014.

The municipality of Sinop, MT has a territorial extension of 3,942 km^2 and approximately 135,000 inhabitants. Its population grew by 20% in the last 7 years following the establishment of a large number of industries in the region (IBGE, 2017), leading to a considerable increase in the demand for energy and/or energy transformation processes. The municipality is located in an area of agricultural expansion and, as an important area of agribusiness in the State, it contributes significantly to the high regional and national rates of deforestation and burns (MOURA; ROMANCINI, 2013).

Because aerosols can be transported over long distances, depending on the regional circulation and the amount and intensity of fires (which are most prevalent during the dry season), aerosols originating in the Amazon region can cause changes at a local scale and in areas that are thousands of kilometers away from the emission regions (PRINS et al., 1998; ARTAXO et al., 2006; OLIVEIRA; MARIANO, 2014). In view of these effects, an area of influence with a radius of 250 km was drawn around the study point (Figure 1). This area, which encompasses 41 cities and has fairly consistent phytophysiognomy and relief, was chosen to represent the Cerrado-Amazon transition region.

Figure 1 – Area of influence established for Sinop, MT, Brazil

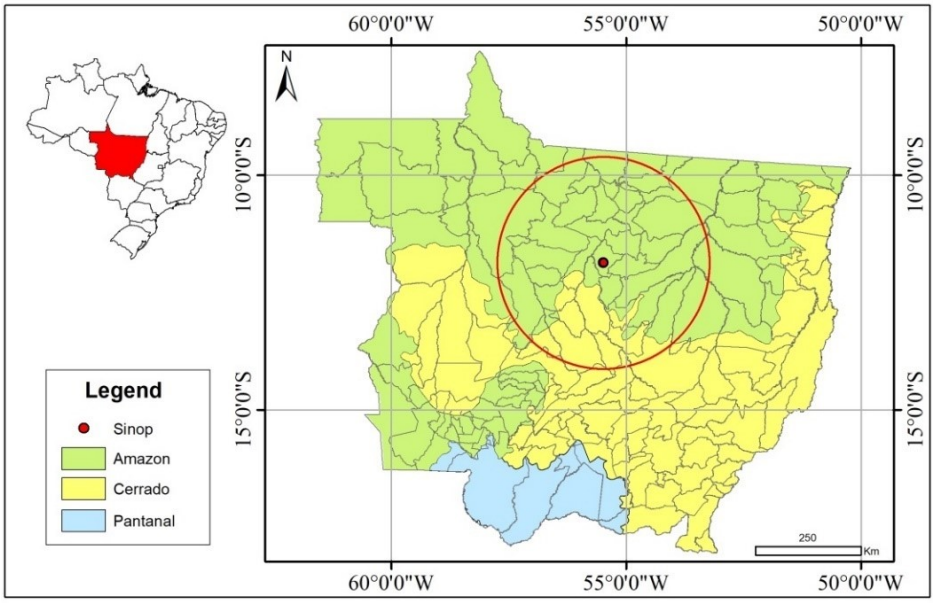

Source: Authors

The region's climate, according to the Köppen climate classification, is tropical hot and humid, Aw, characterized by the presence of two well defined seasons: rainy (October to April) and dry (May to September). Average monthly temperatures range between 23.0°C and 25.8°C, with an annual average of 24.7°C. The region experiences 1900 mm yr^{-1} of precipitation annually, with 70% of total rainfall occurring between November and March (summer) particularly in January, February, and March (SOUZA et al., 2013).

2.2 Instrumentation and measurements

Global and diffuse radiation were monitored by CM3 pyranometers (Kipp & Zonen) placed at a height of 1 m. The pyranometers have a sensitivity response of ± 10–35 $\mu V/Wm^{-2}$, a response time of 18 s, a temperature response of ± 1.0% for the range of −40 °C to 80 °C, and detours to the cosine effect of ± 2% (0 < z < 80). The station is also equipped with following sensors: a Licor at 2 m height for measuring photosynthetically active radiation (PAR), an anemometer at 10 m height for measuring wind speed and direction (03002-L RM YOUNG), a psychrometer at 2 m height with a thermometer shelter (Vaisala, CS 215), a rain gauge (Vaisala, TE 525) at 1.5 m height, and a heliograph at 1.5 m height.

Data acquisition was carried out by a CR1000 datalogger (Campbell Scientific) with an operating frequency of 1 Hz and a sampling rate of 300 readings (5 min).

The diffuse radiation was measured by the MEO shadow ring. The sensor-ring distance and the width of the shadow ring projected onto the equipment were determined from Oliveira et al. (2002) as follows:

$$r = \frac{R}{cos(\delta)}\left[\frac{cos(\varphi)\,cos(\delta)}{cos(\varphi+\delta)}\right] \quad (1)$$

$$w = \frac{b\,cos(\delta)}{cos(\varphi+\delta)} \quad (2)$$

Where: r is the sensor-ring distance (m), R is the shadow ring radius (m), δ is the solar declination, φ is the local latitude, w is the width of the shadow (m), and b is the ring width (m).

The solar radiation data were analyzed to investigate the inconsistencies generated by the data collection and storage system. Daily irradiation measurements were obtained by integration of instantaneous partition (IQBAL, 1983). The data were processed to obtain the moments of sunrise and sunset, solar declination, irradiation at the top of the atmosphere, cosine of the zenith angle (cos Z), and hour angle to the horizontal surface. The diffuse radiance data measured by the MEO shadow ring were corrected using the following geometrical and astronomical correction factors proposed by Oliveira et al. (2002):

$$Fc = \frac{1}{1-Fp} \quad (3)$$

$$Fp = \left(\frac{2b}{\pi R}\right)cos(\delta)\left[\frac{cos(\phi+\delta)}{cos(\delta)}\right]^2 \int_0^{ws} cos(\theta z)\,d\omega \quad (4)$$

Where: b is the ring width (0.1 m), R is the ring radius (0.4 m), ω is the hour angle, and θz is the zenith angle.

The correction factors discussed thus far do not address the atmospheric effects (turbidity, cloudiness, water vapor, and pollution) that are primarily responsible for the anisotropy of the diffuse radiation (IQBAL, 1983; LEBARON et al., 1990; DAL PAI et al., 2016).

The atmospheric transmissivity coefficient of global radiation (K_T) or clearness index was obtained by the ratio of the global radiation (H_G) and radiation at the top of the atmosphere (H_0). Therefore, anisotropic corrections were applied using K_T, taking into account the anisotropic behavior of the dispersion caused by the interaction of solar radiation with the atmosphere. These corrections were proposed by Dal Pai et al. (2016) and depend on atmospheric transmissivity in accordance with the classification of sky coverage described by Escobedo et al. (2009) (Table 1).

Table 1 – Anisotropy correction factors of the diffuse radiation measured by the MEO shadow ring method (Source: Escobedo et al., 2009).

K_T interval	Sky coverage	Correction factor
$0 \leq K_T < 0.35$	Cloudy	0.975
$0.35 \leq K_T < 0.55$	Partially diffuse	1.034
$0.55 \leq K_T < 0.65$	Partially clear	1.083
$K_T \geq 0.65$	Clear	1.108

Next, the classification of sky coverage condition as a function of K_T was established as proposed by Escobedo et al. (2009). This classification uses the sky conditions shown in Table 1 but does not use direct and/or diffuse radiation data. Finally, the frequency distribution of sky coverage conditions was determined.

The geographic and astronomical effects on the evaluation of solar radiation behavior can be minimized by using fractions or radiometric indices. This technique requires that the components of the radiation are obtained in the same place and at same time interval. The radiometric fractions Kd and Kd' are given by the ratio of the diffuse and global radiation and the ratio of diffuse radiation and at the top of the atmosphere, respectively.

3 RESULTS AND DISCUSSION

3.1 Meteorological variables

Figure 2 shows monthly mean values for air temperature, relative humidity, insolation, and precipitation for Sinop, MT from 06/02/2011 to 12/31/2014.

Figure 2 – Monthly averages of (A) air temperature, (B) relative humidity, (C) accumulated rainfall, and (D) sunshine hours for Sinop, MT from 06/02/2011 to 12/31/2014

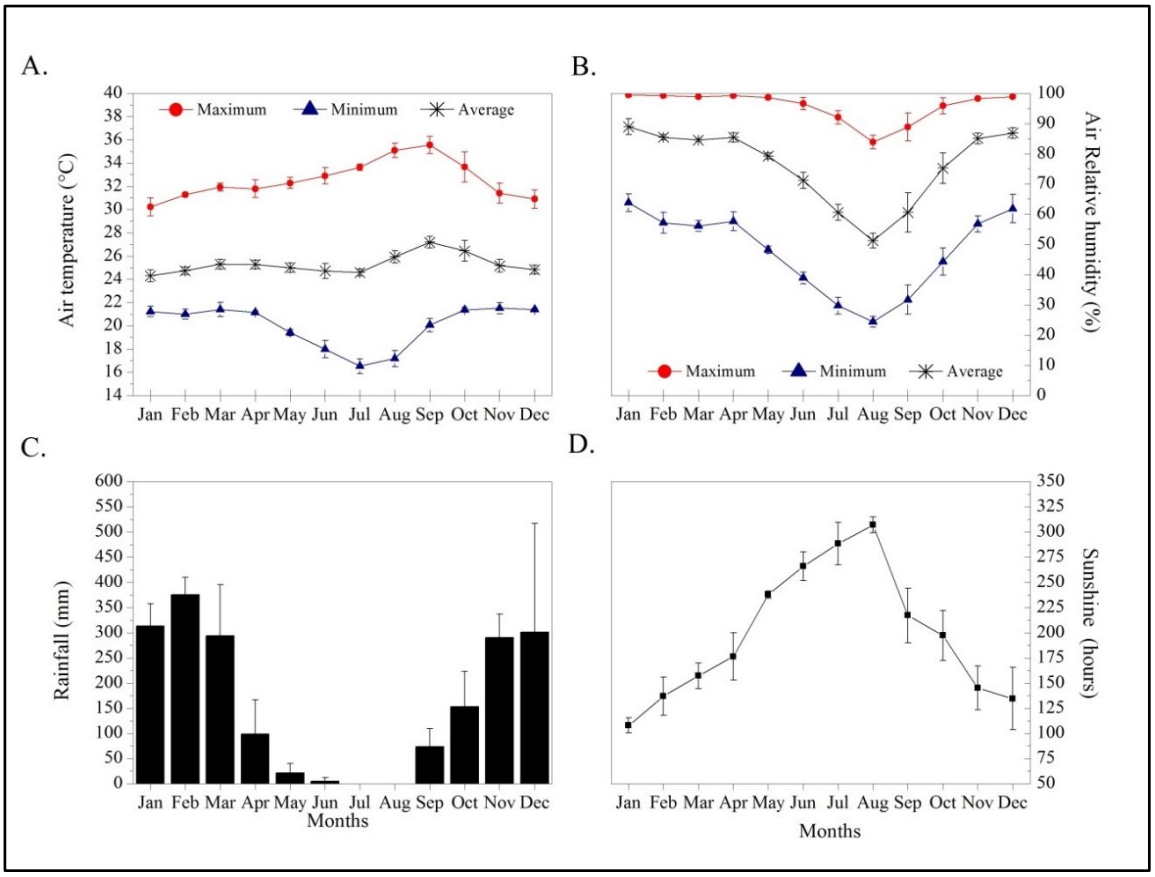

During the study period, the month of February was the wettest on average, with an average rainfall of 375.25 mm, and as expected, the dry season from May to September was characterized by very low rainfall in comparison. The greater variability in precipitation (Figure 1C) in the months of March and December are due to anomalously high monthly totals in 2014 and 2013, respectively. Annual total precipitation in 2012, 2013, and 2014 was 1616.26, 2455.40, and 1776.20 mm, respectively. Sunshine hours were highest in August (307.21 hours) and lowest in January (108.10 hours) (Figure 1D).

The lowest daily temperatures occur during the rainy season (the summer) due to the high concentrations of water vapor in the atmosphere, because water vapor strongly attenuates solar radiation. Correspondingly, the monthly averages of both temperature and sunshine hours are higher in the dry season,

when the weather conditions allow the most sunlight through to the Earth's surface.

Figure 3 shows the monthly total fire spots recorded for Sinop, MT and its area of influence from June 2011 to December 2014. The fire spot data were obtained from the Fire Monitoring database (ProCerrado Program) of the Brazilian Institute of Space Research (INPE/MCTI/MMA). Fire spots were most numerous in September, both in the municipality and in its area of influence.

Figure 3 – Monthly total fire spots in Sinop, MT (B) and its area of influence (A), from June 2011 to December 2014 (Source: INPE, 2018)

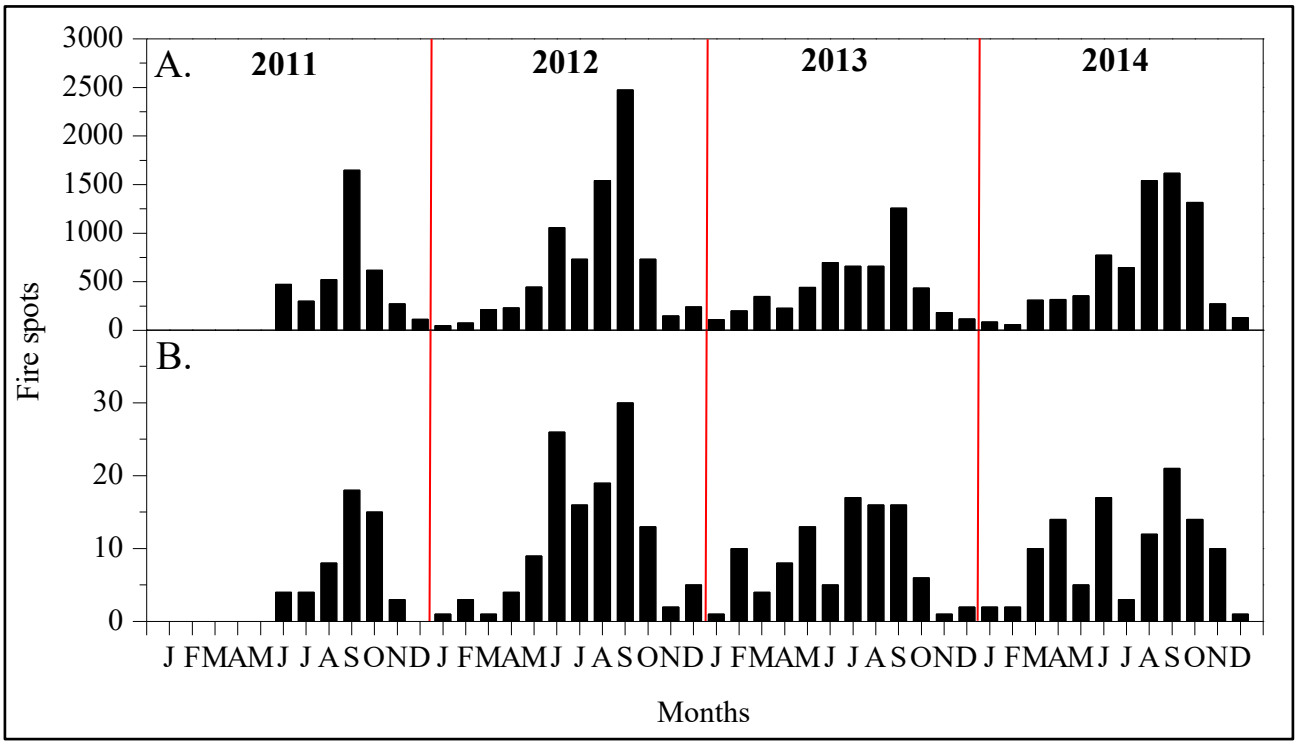

3.2 Seasonality of global and diffuse radiation

Figure 4 shows the geometric relationship that exists between the shadow ring and the projected shadow, as well as monthly averages of the correction factor (Fc) for the latitude of Sinop, MT. The maximum Fc value of 1.198 occurs on 02/21 and 10/17 (solar culmination), while the minimum Fc value of 1.086 occurs on 06/20 (winter solstice). A study conducted by Oliveira et al. (2002a) with three types of

correction factors using the same MEO shadow ring method, in Botucatu, São Paulo State, Brazil (22.90°S and 48.45°W) found that the Fc ranges from a maximum of 1.24 in the summer (01/19 and 11/14) to a minimum of 1.05 at the winter solstice and concluded that this behavior is related to the annual cycle in the sensor-ring distance. In the studies conducted in Botucatu, the ratio of sensor-ring distance and radius ranges from 0.92 in summer to 1.33 in winter. In the Sinop, MT region it was found to range between 0.98 in the summer and 1.20 in winter (Figure 3A), indicating that these differences may arise from differences in the radius and width of the rings of the different models. Overall, this comparison shows that this shadow ring model displays similar performance for routine measurements in other climatic regions, allowing for the dependence of the measures of diffuse radiation on the specific geometry factors of measurement equipment as well as astronomical, geographical, and atmospheric factors.

Figure 4 - Relationship between sensor-ring distance and shadow ring radius (r/R) (A) and relationship between shadow and ring width (w/b) and (B) monthly averages of correction factor (Fc) for Sinop, MT, from 06/02/2011 to 12/31/2014

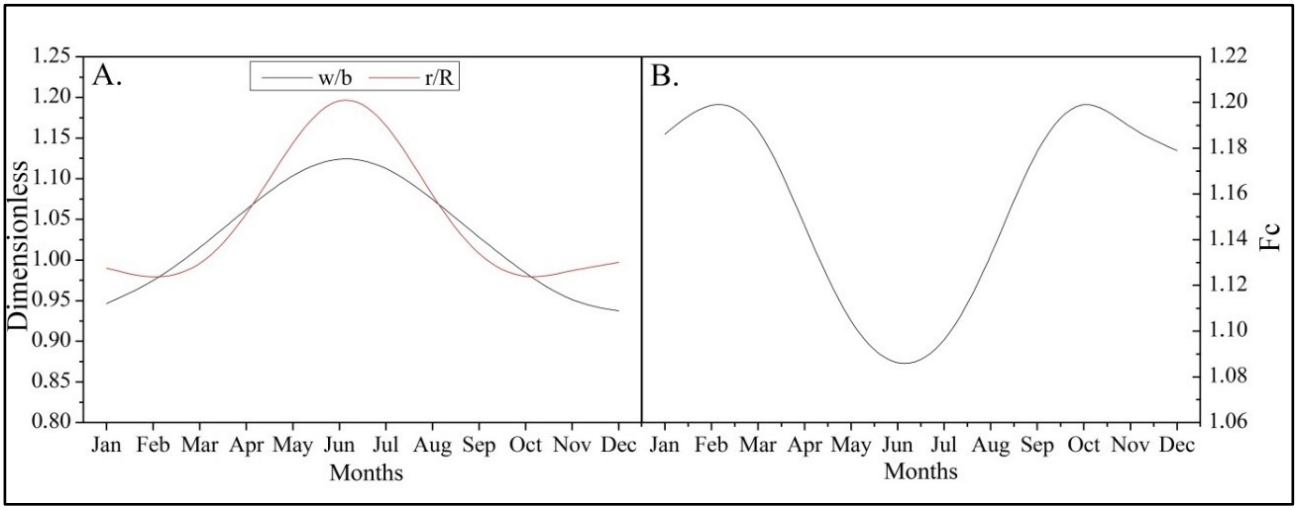

The daily variations in global and diffuse radiation reaching the horizontal surface can be seen in Figure 5. In contrast to global radiation, diffuse radiation has higher values during the rainy season. The daily values of diffuse radiation ranged

from 1.74 MJ m^{-2} d^{-1} (K_T = 0.77, on 06/25/2014) to 11.25 MJ m^{-2} d^{-1} (K_T = 0.54, on 02/29/2012).

The average daily value of global radiation observed during the study period was 19.26 MJ m^{-2} d^{-1}, with oscillations between 2.15 MJ m^{-2} d^{-1} (K_T = 0.05, 12/23/2013) and 29.83 MJ m^{-2} d^{-1} (K_T = 0.75 on 12/18/2012). In December (rainy season), most days were characterized by high cloudiness. Local rainfall is usually due to convective formation processes, which predominate in the afternoon and evening and are characterized by large spatial variability and high intensity. During the summer (rainy season), clear skies tend to be associated with high atmospheric transmissivity of solar radiation due to the low atmospheric concentrations of water vapor and suspended particulate matter (QUERINO et al., 2011). The daily average values of global radiation in spring, summer, autumn, and winter were 18.68, 18.45, 18.70, and 21.24 MJ m^{-2}, respectively.

Figure 5 – Daily levels of global and diffuse radiation (MJ m−2 d−1) in Sinop, MT from 06/02/2011 to 12/31/2014

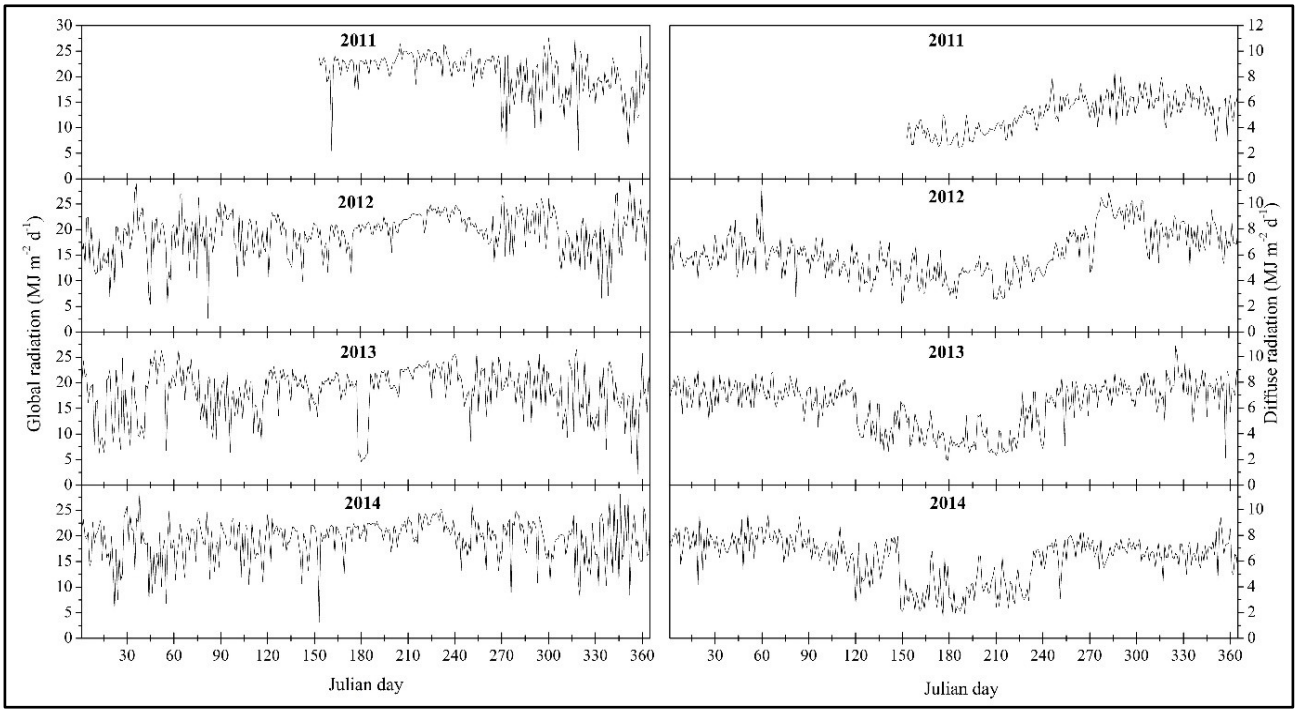

3.3 Radiometric fractions

Figures 6 and 7 shows the monthly averages of global radiation (H_G), diffuse radiation (H_D), and atmospheric transmissivity coefficient (K_T). Overall, H_G has higher values during the dry period and lower values during the rainy period, with averages of 22.75 ± 0.61 MJ m^{-2} d^{-1} in August and 16.44 ± 1.45 MJ m^{-2} d^{-1} in January. However, the decline from August to October is not symmetrical, as the average value in September (20.03 MJ m^{-2} d^{-1}) is not higher than in October (20.11 MJ m^{-2} d^{-1}). This behavior is a result of the increased concentration of biomass burning aerosols in the atmosphere in September due to the high number of fire spots in the region at this time of year (Figure 3). In addition to the high fire activity in the State, there is also long-distance transport of aerosols from northern Brazil (PALÁCIOS et al., 2018). The biomass burning aerosols modify the radiative balance at the surface by absorbing and scattering the solar radiation. The increase in biomass burning aerosols thus leads to a relative increase in diffuse radiation, which in turn can affect many biological processes such as plant productivity (PAULIQUEVIS et al., 2007; MERCADO et al., 2009).

Figure 6 - Monthly averages of global radiation (H_G) (A) and of diffuse radiation (H_D) (B) in the region of Sinop, MT, between 06/02/2011 and 12/31/2014

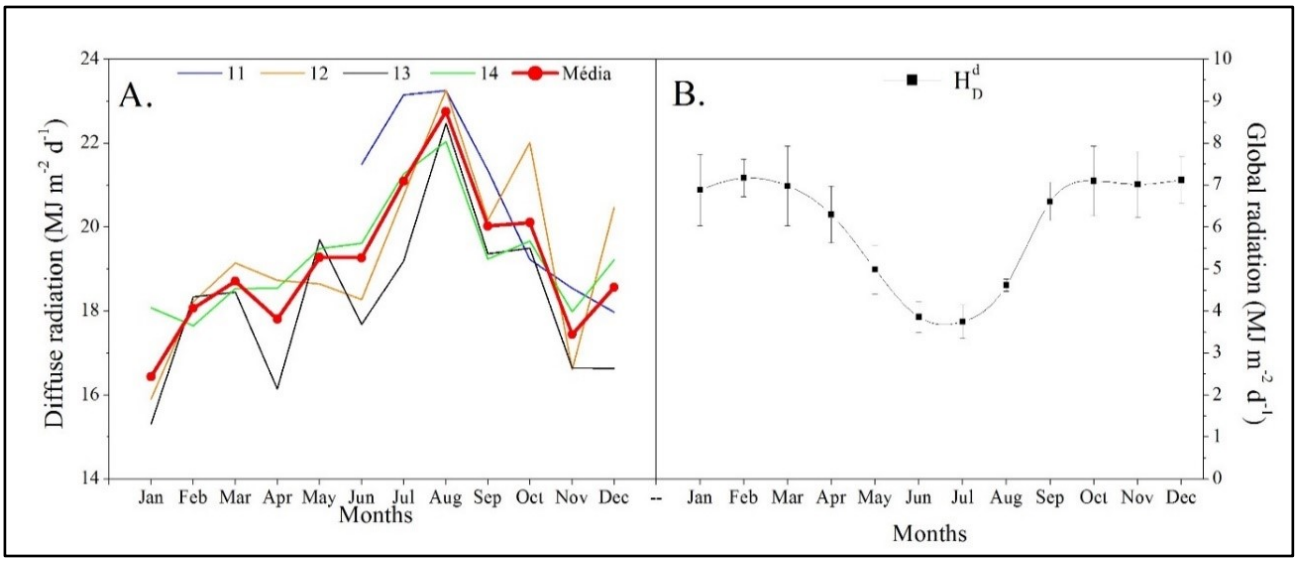

Figure 7 - Monthly averages of the atmospheric transmissivity coefficient (K_T) in the Sinop, MT region, between 06/02/2011 and 12/31/2014

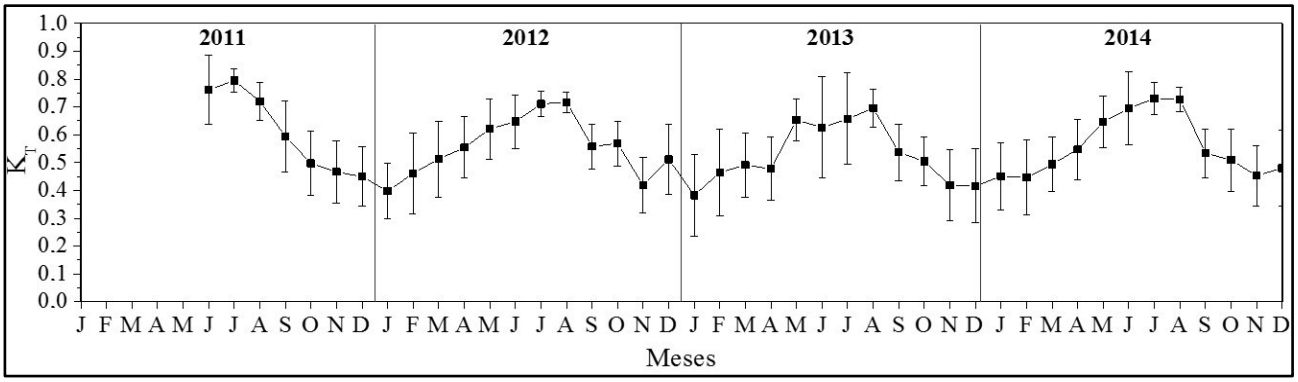

The seasonality of the diffuse component is similar to that of the radiation at the top of the atmosphere, but the diffuse component is strongly affected by the geometric correction, which in turn is dependent on the zenithal angle. However, the annual cycle of diffuse radiation is also dependent on weather conditions (specifically, cloudiness and precipitation), as evidenced by the increase in standard deviations for the rainy months and the great variability in observed sky cover classes.

The diffuse radiation has isotropic and anisotropic characteristics that result from atmospheric scattering. In general, when concentrations of water vapor are high (i.e., in summer), the solar radiation is attenuated by reflection and anisotropic diffusion. However, since the radiation is transmitted, there is an inversion process of the diffuse radiation between the cloud and the surface, wherein scattering with isotropic characteristics is generated. In turn, in the dry season isotropic and anisotropic scattering occur together (CHWIEDUK, 2009; POSADILLO; LUQUE, 2009; SOUZA et al., 2012; SOUZA; ESCOBEDO, 2013; DAL PAI et al., 2016).

The highest daily average values of diffuse radiation occurred between October (7.10 ± 0.83 MJ m^{-2} d^{-1}) and April (6.30 ± 0.68 MJ m^{-2} d^{-1}), with a maximum in February (7.17 MJ m^{-2} d^{-1}, equivalent to 39.69% H_G). The lowest average values were observed in July (3.75 MJ m^{-2} d^{-1} or 17.79% H_G). The standard deviations on the monthly averages of diffuse radiation vary from 0.15 in August to 0.95 MJ m^{-2} d^{-1} in March. The highest standard deviations occur in spring and fall, the transitional seasons. This behavior

matches the results of studies conducted in other regions of Brazil such as Cascavel (DRECHMER; RICIERI, 2006), and indicates that in general, in the North of Mato Grosso (the Cerrado-Amazon transition region), the winter is characterized by clear sky days and the summer by cloudy sky days, in keeping with the hydrological conditions in the region.

This evaluation of the frequency of occurrence of the daily values of K_T throughout the year (Table 2) highlights the effect of atmospheric composition (clouds, water vapor, and aerosols) on the transmission of global radiation and the behavior of diffuse radiation. During the dry season clear (62.07%) and partially clear (23.45%) sky days occur more frequently, while in the rainy season partially diffuse sky conditions prevail (51.47%). In January, the rainy season, cloudy (36.56%), and partially diffuse (50.54%) days occur more frequently, whereas in August 97.58% of the days are characterized by atmospheric transmissivity higher than 55%. This behavior is similar to that seen by Teramoto; Escobedo (2012) in Botucatu, SP.

Table 2 – Frequency of sky conditions in Sinop, MT during the period 06/02/2011–12/31/2014) according to the classification proposed by Escobedo et al. (2009)

Month	Sky coverage conditions (%)			
	I (cloudy)	II (partially diffuse)	III (partially clear)	IV (clear)
January	36.56	50.54	12.90	0.00
February	22.41	50.49	21.22	5.87
March	11.83	52.69	27.96	7.53
April	10.00	44.44	31.11	14.44
May	1.08	13.98	29.03	55.91
June	5.03	5.00	12.56	77.41
July	2.42	1.61	8.87	87.10
August	0.00	2.42	20.97	76.61
September	3.33	24.17	36.67	35.83
October	6.45	45.97	41.13	6.45
November	25.00	58.33	15.00	1.67
December	15.48	57.80	19.44	7.28

Sky coverage II (partially diffuse) conditions were observed more frequently during the rainy months, as were sky coverage I conditions. The frequency of sky coverage III conditions values ranged from 41.13% in October to 8.87% in July. Overall, during the period studied, sky coverage classes of I to IV prevailed in the Sinop, MT

region 11.63%, 33.95%, 23.07%, and 31.31% of the time, respectively. These values correspond to a high percentage of days (54.41%) with K_T greater than 0.55.

The daily mean values of the radiometric fractions of diffuse radiation Kd and Kd' varied throughout the year (Figure 8) according to astronomical variations and the atmospheric composition. In general, the highest values occur in the rainy or transition seasons. During these periods, the diffuse radiation can be equivalent to 54% (January/13) and 32% (March/12) of global radiation (Kd), and, 18% (November/13) to 12% (January/12) of radiation at the top of the atmosphere (Kd'). The lowest values of these two radiometric fractions occur between May and August and decrease over that time period, with Kd decreasing from 0.31 in May to 0.16 in July and Kd' decreasing from 0.15 in May to 0.10 in July.

Figure 8 – Daily values of radiometric fractions Kd and Kd’ in Sinop, MT, between 06/02/2011 and 12/31/2014

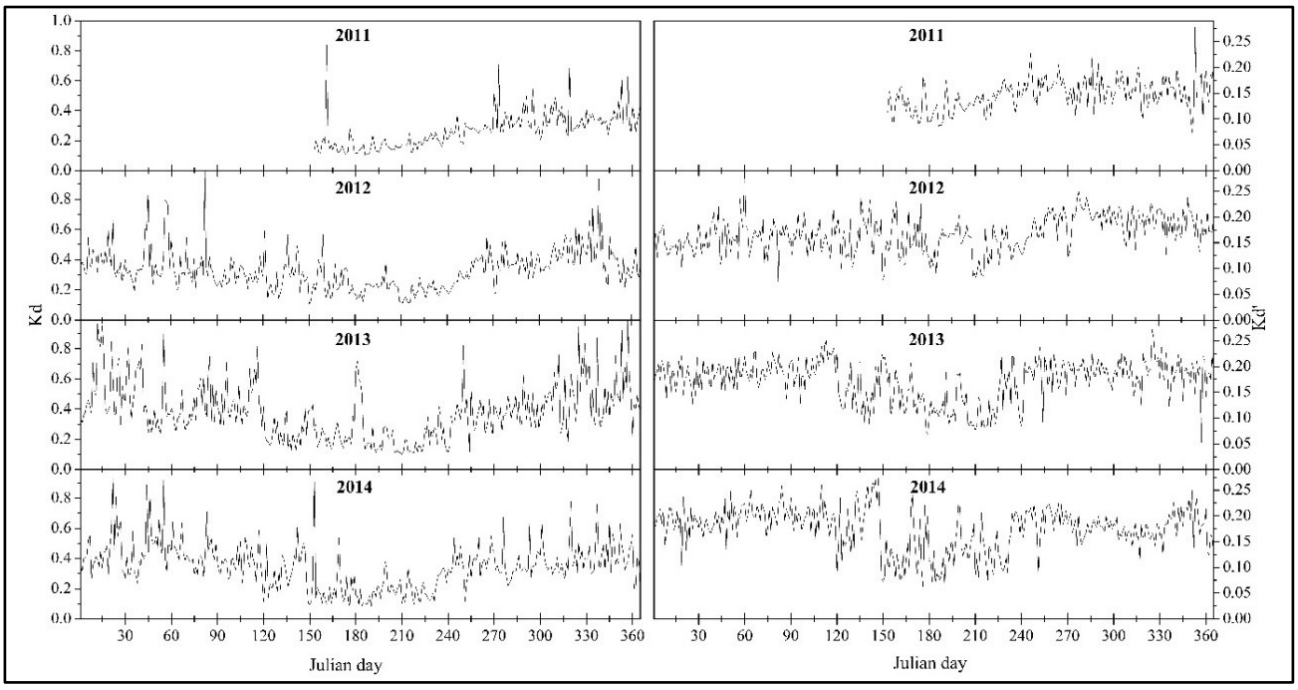

On average, 35.06% of days in the region of Sinop, MT are characterized by partially diffuse sky conditions. The diffuse radiation can represent 8.02%–99.12% of the global radiation and 5.33%–29.01% of the solar energy incident at the top of the atmosphere.

4 CONCLUSIONS

In the Cerrado-Amazon transition region of Mato Grosso state, global radiation shows higher values during the dry season (May to September), while the diffuse radiation presents the opposite behavior, with the highest values occurring during the rainy season (October to April).

The results allow to indicate that the global and diffuse radiation present similar seasonality, depending on the atmospheric conditions. Cloudiness and biomass burning aerosol concentrations influence the transmissivity of global and diffuse radiation, particularly during the transition months between the rainy and dry seasons.

The solar radiation data were also used to compute various climatic parameters including KT and Kd. The results are in good agreement with our previous findings. The study can help to establish a comprehensive solar radiation database for subsequent building engineering and environment evaluations. The direct radiation can be obtained by the difference between global and diffuse for applications in this region. Other studies must be carried out to calibrate the anisotropic coefficients in the region and the development of simplified models of diffuse radiation estimation based on other meteorological variables.

5 ACKNOWLEDGMENTS

The authors are grateful to the Research Support Foundation of Mato Grosso State (FAPEMAT) for the financial support provided by a master's scholarship. The authors are also grateful to the Brazilian Institute of Space Research (INPE) for providing the fire spot data obtained from Fire Monitoring database (ProCerrado Program) and to the Solar Radiometry Laboratory of Botucatu - São Paulo State University.

REFERENCES

ANDRADE, N. L. R. de; AGUIAR, R. G.; SANCHES, L.; ALVES, É. C. R. de F.; NOGUEIRA, J. de S. Partição do saldo de radiação em áreas de Floresta Amazônica e Floresta de transição

Amazônia-Cerrado. **Revista Brasileira de Meteorologia**, São José dos Campos, v. 24, n. 3, p. 346-355, 2009.

ARTAXO, P.; OLIVEIRA, P. H.; LARA, L. L.; PAULIQUEVIS, T. M.; RIZZO, L. V.; PIRES JUNIOR, C.; PAIXÃO, M. A.; LONGO, K. M.; FREITAS, S.; CORREIA, A. L. Efeitos climáticos de partículas de aerossóis biogênicos e emitidos em queimadas na Amazônia. **Revista Brasileira de Meteorologia**, São José dos Campos, v. 21, n. 3a, p. 168-22, 2006.

BORGES, V. P.; OLIVEIRA, A. S.; COELHO FILHO, M. A.; SILVA, T. S. M.; PAMPONET, B. M. Avaliação de modelos de estimativa da radiação solar incidente em Cruz das Almas, Bahia. **Revista Brasileira de Engenharia Agrícola e Ambiental**, Campina Grande, v. 14, n. 1, p. 74-80, 2010.

CHWIEDUK, D. A. Recommendation on modeling of solar energy incident on a building envelope. **Renewable Energy**, Oxford, v. 34, n. 3, p. 736-741, 2009.

CODATO, G.; OLIVEIRA, A. P.; SOARES, J.; ESCOBEDO, J. F.; GOMES, E. M.; DAL PAI, A. Global and diffuse solar irradiances in urban and rural areas in Southeast Brazil. **Theoretical and Applied Climatology**, Wien, v. 93, n. 1, p. 57-73, 2008.

CRUZ, T.; SCHAEFFER, R.; LUCENA, A. F. P.; MELO, S.; DUTRA, R. Solar water heating technical-economic potential in the household sector in Brazil. **Renewable Energy**, Oxford, v. 146, p. 1618-1639, 2020.

DAL PAI, A.; ESCOBEDO, J. F.; DAL PAI, E.; OLIVEIRA, A. P.; SOARES, J. R.; CODATO, G. MEO shadowring method for measuring diffuse solar irradiance: Corrections based on sky cover. **Renewable Energy**, Oxford, v. 99, p. 754-763, 2016.

DAL PAI, A.; ESCOBEDO, J. F.; DAL PAI, E.; SANTOS, C. M. Estimation of hourly, daily and monthly mean diffuse radiation based on MEO sahdowring corrections. **Energy Procedia**, Amsterdam, v. 57, p. 1150-1159, 2014.

DRECHMER, P. A. O.; RICIERI, R. P. Irradiação global, direta e difusa, para a região de Cascavel, Estado do Paraná. **Acta Scientiarum Technology**, Maringá, v. 28, n. 1, p. 73-77, 2006.

ESCOBEDO, J. F.; GOMES, E. N.; OLIVEIRA, A. P.; SOARES, J. Modeling hourly and daily fractions of UV, PAR and NIR to global solar radiation under various sky conditions at Botucatu, Brazil. **Applied Energy**, London, v. 86, n. 3, p. 299-309, 2009.

FURLAN, C.; OLIVEIRA, A. P.; SOARES, J.; CODATO, G.; ESCOBEDO, J. F. The role of clouds in improving the regression model for hourly values of diffuse radiation. **Applied Energy**, London, v. 92, n. 2, p. 240-254, 2012.

INSTITUTO BRASILEIRO DE GEOGRAFIA E ESTATÍSTICA [Internet]. Brasília: Ministério do Planejamento, Orçamento e Gestão (BR) [cited 2017 feb 27]. **Cidades**. Available from: https://cidades.ibge.gov.br/brasil/mt/sinop/panorama

INSTITUTO NACIONAL DE PESQUISAS ESPACIAIS [Internet]. São José dos campos: **Portal do Monitoramento de Queimadas e Incêndio**, Platform of Monitoring and Warning of Forest Fires in the Cerrado. 2018. Available from: http://www.dpi.inpe.br/proarco/bdqueimadas

IQBAL M. An introduction to solar radiation. **Academic Press**, Canadá, 1983. 390 p.

LeBARON, B. A.; MICHALSKY, J. J.; PEREZ, R. A simple procedure for correcting shadowband data for all sky conditions. **Solar Energy**, Kidlington, v. 44, n. 5, p. 249-56, 1990.

MARTINS, F. R.; PEREIRA, E. B.; SILVA, S. A. B.; COLLE, S. Solar energy scenarios in Brazil, Part one: resource assessment. **Energy Policy**, Kidlington, v. 36, n. 8, p. 2853-2864, 2008.

MELO, J. M. D. **Desenvolvimento de um sistema para medir simultaneamente radiações global, difusa e direta** [Thesis]. Botucatu: Faculdade de Ciências Agronômicas, Universidade Estadual Paulista. 1994. 193 p.

MERCADO, L. M.; BELLOUIN, N.; SITCH, S.; BOUCHER, O.; HUNTINGFORD, C.; WILD, M.; COX, P. M. Impact of changes in diffuse radiation on the global land carbon sink. **Nature**, London, v. 458, n. 7241, p. 1014-1017, 2009.

MOURA, E. D. de; ROMANCINI, S. R. Espacialidade das manifestações culturais na cidade: O caso de Sinop – MT. In: COLÓQUIO DO NÚCLEO DE ESTUDOS EM ESPAÇO E REPRESENTAÇÕES, 5., 2013, Cuiabá. **Anais**... Cuiabá: UFMT, 2013. ISSN 1981-6820.

OLIVEIRA, A. P.; ESCOBEDO, J. F.; MACHADO, A. J. A new shadow-ring device for measuring diffuse solar radiation at surface. **Journal of Atmospheric and Oceanic Technology**, Boston, v. 19, n. 5, p. 698-708, 2002.

OLIVEIRA, A. M.; MARIANO, G. L. Identificação de entrada de plumas de queimada e principais áreas afetadas na região Sul do Brasil. **Ciência e Natura**, Santa Maria, v. 36, n. 2, p. 241-249, 2014.

PALÁCIOS, R. S.; SALLO, F. S.; MARQUES, J. B.; SANTOS, A. C. A.; MENEZES, J. A.; BIUDES, M. S.; NOGUEIRA, J. S. Variabilidade espaço-temporal da profundidade ótica de aerossóis nos biomas cerrado e pantanal da região central do Brasil. **Nativa**, Sinop, v. 6, n. 1, p. 56-65, 2018.

PAULIQUEVIS, T.; ARTAXO, P.; OLIVEIRA, P. H.; PAIXÃO, M. O papel das partículas de aerossol no funcionamento do ecossistema amazônico. **Ciência e Cultura**, Campinas, v. 59, n. 3, p. 48-50, 2007.

PEREIRA, E. B.; MARTINS, F. R.; ABREU, S. L.; RÜTHER, R. **Atlas brasileiro de energia solar**. São José dos Campos: INPE, 2006. 60 p.

PIACENTINI, R. D.; SALUM, G. M.; FRAIDENRAICH, N.; TIBA, C. Extreme total solar irradiance due to cloud enhancement at sea level of the NE Atlantic coast of Brazil. **Renewable Energy**, Oxford, v. 36, n. 1, p. 409-412, 2011.

POSADILLO, R.; LUQUE, R. L. Hourly distributions of the diffuse fraction of global solar irradiation in Córdoba (Spain). **Energy Conversion and Management**, Oxford, v. 50, n. 2, p. 223-231, 2009.

ROSSI, F. S.; SANTOS, G. A. de A. Fire dynamics in Mato Grosso State, Brazil: the relative roles of gross primary productivity. **Big Earth Data**, London, v. 4, n. 1, p. 23-44, 2020.

PRINS, E. M.; FELTZ, J. M.; MENZEL, W. P.; WARD, D. E. An overview of GOES-8 diurnal fire and smoke results for SCAR-B and 1995 fire season in South America. **Journal of Geophysical Research**, Washington, v. 103, n. D24, p. 31821-31835, 1998.

QUERINO, C. A. S.; MOURA, M. A. L.; QUERINO, J. K. A. S.; VON RADOW, C.; MARQUES FILHO, A. O. Estudo da radiação solar global e do índice de transmissividade (Kt), externo e interno, em uma floresta de mangue em Alagoas-Brasil. **Revista Brasileira de Meteorologia**, São José dos Campos, v. 26, n. 2, p. 204-294, 2011.

RELVA, S. G.; GIMENES, A. L. V.; UDAETA, M. E. M.; GALVÃO, L. C. R. Transmittance index characterization at two solar measurement stations in Brazil. **Theoretical and Applied Climatology**, Wien, v. 139, n. 1-2, p. 205-219, 2019.

SALAZAR, G.; GUEYMARD, C.; GALDINO, J. B.; VILELA, O. de C.; FRAIDENRAICH, N. Solar irradiance time series derived from high-quality measurements, satellite-based models, and reanalyses at a near-equatorial site in Brazil. **Renewable and Sustainable Energy Reviews**, Amsterdam, v. 117, e109478, 2020.

SILVA, G. D. P. da; SHARQAWY, M. H. Techno-economic analysis of low impact solar brackish water desalination system in the Brazilian Semiarid region. **Journal of Cleaner Production**, Amsterdam, v. 248, e119225, 2020.

SOUZA, A. P.; ESCOBEDO, J. F.; DAL PAI, A.; GOMES, E. N. Annual evolution of global, direct and diffuse radiation and fractions in tilted surfaces. **Engenharia Agrícola**, Jaboticabal, v. 32, n. 2, p. 247-260, 2012.

SOUZA, A. P.; MOTA, L. L.; ZAMADEI, T.; MARTIM, C. C.; ALMEIDA, F. T.; PAULINO, J. Classificação climática e balanço hídrico climatológico no Estado de Mato Grosso. **Nativa**, Sinop, v. 1, n. 1, p. 34-43, 2013.

SOUZA, A. P.; ESCOBEDO, J. F. Estimativas das radiações direta e difusa em superfícies inclinadas com base na razão de insolação. **Revista Brasileira de Ciências Agrárias**, Recife, v. 8, n. 3, p. 492-502, 2013.

SOUZA, A. P.; ZAMADEI, T.; MONTEIRO, E. B.; CASAVECCHIA, B. H. Transmissividade Atmosférica da Radiação Global na Região Amazônica de Mato Grosso. **Revista Brasileira de Meteorologia**, São José dos Campos, v. 31, n. 4 suppl., p. 639-648, 2016.

TERAMOTO, E. T.; ESCOBEDO, J. F. Análise da frequência anual das condições de céu em Botucatu, São Paulo. **Revista Brasileira de Engenharia Agrícola e Ambiental**, Campina Grande, v. 16, n. 9, p. 985-992, 2012.

VIANA, T. S.; RUTHER, R.; MARTINS, F. R.; PEREIRA, E. B. Assessing the potential of concentrating solar photovoltaic generation in Brazil with satellite-derived direct normal irradiation. **Solar Energy**, Kidlington, v. 85, n. 3, p. 486-495, 2011.

AUTHORSHIP CONTRIBUTIONS

1 - Tamara Zamadei
Programa de Pós-Graduação em Física Ambiental da Universidade Federal de Mato Grosso. Engenheira Florestal, Mestre em Ciências Ambientais e Doutora em Física Ambiental
https://orcid.org/0000-0001-7341-2514 – tamarazamadei@hotmail.com
Contribution: data curation; formal analysis; resources; validation; writing – original draft

2 - Adilson Pacheco de Souza
Instituto de Ciências Agrárias e Ambientais da Universidade Federal de Mato Grosso, Campus Universitário de Sinop. Engenheiro Agrícola, Mestre e Doutor em Agronomia (Irrigação e Drenagem)
https://orcid.org/0000-0003-4076-1093 – pachecoufmt@gmail.com
Contribution: Conceptualization; data curation; Project administration; resources; supervision; writing – review & editing.

3 - Frederico Terra de Almeida
Instituto de Ciências Agrárias e Ambientais da Universidade Federal de Mato Grosso, Campus Universitário de Sinop. Engenheiro Civil, Mestre em Engenharia Agrícola e Doutor em Produção Vegetal.
https://orcid.org/0000-0003-1055-5766 – fredterr@gmail.com
Contribution: funding acquisition; investigation; writing – review & editing.

4 - João Franscisco Escobedo
Faculdade de Ciências Agronômicas da Universidade Estadual Paulista, Campus de Botucatu. Físico, Mestre em Energia Nuclear e Doutor em Física.
https://orcid.org/0000-0002-8196-4447 – escobedo@fca.unesp.br
Contribution: funding acquisition; investigation; methodology; software.

HOW TO QUOTE THIS ARTICLE

ZAMADEI, T.; SOUZA, A. P.; ALMEIDA, F. T.; ESCOBEDO, J. F. Daily Global and diffuse radiation in the Brazilian Cerrado-Amazon transition region. Ciência e Natura, Santa Maria, v. 43, e37, p. 1-20, 2021. DOI: https://doi.org/10.5902/2179460X39775. Accessed: Month Abbreviated. day, year.